

Short Communication

The Influence of Mica Iron Oxide Pigments on Epoxy Coating Properties Prepared on AISI 1045 Steel Rebar Immersed in 3.5 wt% NaCl Solution

Yongzhi He, Bo Zhou *

College of Architecture & Environment, Sichuan University, Chengdu, Sichuan, 610065, China

*E-mail: zxt001@163.com

Received: 19 March 2021/ Accepted: 9 May 2021 / Published: 31 May 2021

The use of anti-corrosion pigments in organic coatings significantly increases corrosion resistance of steel rebars. In this study, different ratios of mica iron oxide (MIO) pigments were added to the structure of epoxy resin (ER)-based primer coatings. The prepared coating materials were applied to samples of AISI 1045 steel rebars with 8 mm diameter and their corrosion resistance was investigated using EIS and polarization tests. The corrosion potential and resistance of steel rebars coated with ER containing 10 wt% MIOs (10MIO) were found to be higher than the other samples in the EIS. Polarization results exhibited that except the MIO-free sample, all coated steel rebars stayed in the passive level in the experiment procedure which exhibited their excellent resistance to AISI 1045 steel corrosion in marine medium. Surface morphology of coated steel rebar showed that the 10MIO sample had less pitting corrosion than the other tests, which matched the electrochemical findings.

Keywords: ER coatings; Mica iron oxide; Electrochemical corrosion resistance; Reinforced concrete

1. INTRODUCTION

Corrosion of reinforced concrete is an undeniable fact that in most cases is caused by the penetration of chlorine or carbon dioxide and the destruction of the alkaline environment of concrete [1, 2]. Due to the good mechanical properties of steel, reinforced concrete is usually made of steel. However, in terms of corrosion resistance, steel has a weakness and therefore the use of coatings along with cathodic protection is inevitable in most cases [3, 4].

The primer plays a special role in the adhesion of synthetic elastic bands to the substrate (steel rebar), preventing corrosion and protecting and maintaining the steel rebars [5, 6]. The primer is applied as the first layer on the surface. A layer of primer is applied as an anti-corrosion and adhesive tape to the surface of the steel rebar, which usually contains structures containing polymers and synthetic elastic compounds, including butyl rubber [7, 8]. ER is a mix of chemical bonds shaped by

cross linking and polymerization [9-11]. Exposure to sunlight, moisture and heat can change the mechanical property of ERs, which should be considered before special engineering use [12].

In the case of the steel reinforcing coatings in concrete structure, the preferred levels of mechanical properties such as tensile strength, yield strength and modulus of elasticity can be attained by controlled curing and appropriate dosage of nanomaterials and organic pigments [13, 14].

Mica iron oxide pigments (MIOs), as one of the most widely used organic pigments with a blocking mechanism, are used within the primer structure as a barrier against the penetration of corrosive agents in anti-corrosion coatings [15]. Mica iron oxide is a chemically neutral substance and rarely reacts with acids, bases, salts and other substances. It is also a non-toxic substance and has good thermal stability, because its melting point is more than 1000 °C. These pigments strengthen the resin matrix and increase adhesion in multilayer coatings. One of the most important properties of these pigments is their ability to prevent the penetration of corrosive agents that cause a difficult and tortuous path against the influence of corrosive agents. In the present study, ER coating modified by MIOs was used as a pigment. The coatings were then applied on a steel rebar to evaluate anti-corrosion performance in the marine environment by using EIS and polarization tests.

2. MATERIALS AND METHODS

The corrosion behaviour of coated steel reinforcement in marine solution was investigated using AISI 1045 steel with an 8mm diameter. The chemical composition of AISI 1045 carbon steel is seen in Table 1.

Table 1. Chemical composition of AISI 1045 carbon steel (wt%)

C	Si	Mn	P	S	Cu	Ni	Cr	Fe
0.43	0.181	0.7	<0.04	<0.05	0.031	8.7	0.025	Residual

Bisphenol A diglycidyl ether as constituent of epoxy resin (DER 331, Dow chemical Co. epoxy value, 0.51-0.55 mol/100g epoxy), the curing agent 4,4'-diaminodiphenylsulfone (DDS) were produced by the Sinopharm Chemical Reagent Company (Shanghai, China). Chemical structure of DER and DDS are shown in figure 1.

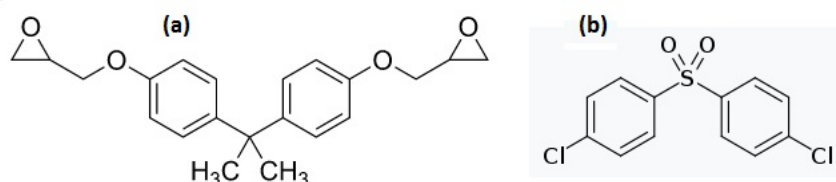


Figure 1. Chemical structure of (a) DER and (b) DDS

DER was stirred at a high-speed mixer for 10 minutes. When the temperature reaches up to 40°C, the DDS agent was added and mixed for 20 minutes. MIO pigments were uniformly dispersed in a single disc bead mill with slurry and dispersing agent, using 1 mm sized glass beads as grinding

media filled up to disc level. The procedure was carried out for another 30 minutes. The process will be repeated until the dispersion is uniform.

Before applying the ER primer, the surface of the steel rebars were cleaned with a wire brush and to ensure complete removal of grease and rust, the surface of the steel was sanded using a soft sandpaper and finally the surfaces were washed with acetone and finally dried with air flow. The ER was applied on the AISI 1045 steel rebar using a draw-down bar. The coatings were then applied to the steel rebars by the filmmaker. The coating was dried and cured in a dust-free environment for one day before testing. After drying the coatings, the final thickness of the dry film was measured using a thickness gauge, which obtained a thickness of $110 \pm 8 \mu\text{m}$.

MIO is a naturally occurring iron oxide that has a lamellar structure similar to mica. The basic properties of MIO are summarized in table 2.

Table 2. Basic properties of MIO

Property	Value
Hardness	6
Electrical conductivity	60 $\mu\text{S}/\text{cm}$
Colour	black
Lamellarity	> 70
Density	5.25 g/cm^3
Melting point	1,539 $^{\circ}\text{C}$
Molar mass	159.687 $\text{g}\cdot\text{mol}^{-1}$
Magnetic susceptibility	+3586.0 $\cdot 10^{-6} \text{cm}^3/\text{mol}$

Different weight ratios of MIO pigments (0, 5, 10, 15 wt%) were used in the ER primer. Complete mixing of primer components was done by a mechanical stirrer at 1000 rpm for 90 minutes.

In this study, Portland cement (PC) was utilized as the binder. Table 3 shows the PC chemical compositions. The water to cement ratio (w/c) for all mixes was kept at 0.45.

Table 3. Chemical compositions of PC

PC	
Al_2O_3	4.32
SiO_2	18.17
Fe_2O_3	2.35
SO_3	2.84
CaO	60.34
Na_2O	0.17
K_2O	0.21

For electrochemical tests, to achieve the cement hydration, the concrete specimens were placed in cylinder molds with a 10cm diameter and 30cm in height for 24 hours at 95% confidence humidity levels and ambient temperature. The steel rebar was positioned vertically in the cylinder's middle.

The corrosion behaviour of coated steel rebars was studied using EIS and polarization resistance techniques. Open circuit potential (OCP) was done through a high-impedance voltmeter through an input resistance. For the tests, a triple-electrode device was used, with a steel bar reinforcement, saturated calomel and a platinum rod as working, reference, and auxiliary electrodes, respectively. The examination was done after being exposed into 3.5wt% NaCl media as a marine environment at different exposure times (1, 2, 4 and 8 weeks). The EIS measurements were performed at a frequency ranges from 0.01Hz to 0.1MHz. The polarization characterizations were done at a scanning rate of 1 mV/s after 4 weeks of immersion time. The surface morphology of specimens was examined using a SEM.

3. RESULTS AND DISCUSSION

The OCP of the rebars coated by ER containing the various concentrations of MIOs are investigated in a salty environment. The changes of the OCP versus exposure time of the specimens are indicated in Figure 2. As shown, the OCP of blank specimen becomes negative at initial days of immersion which can be related to the permeation of corrosive electrolyte under the coatings. The coatings have micro-sized pores and holes which are efficient conductive paths for diffusion of electrolyte.

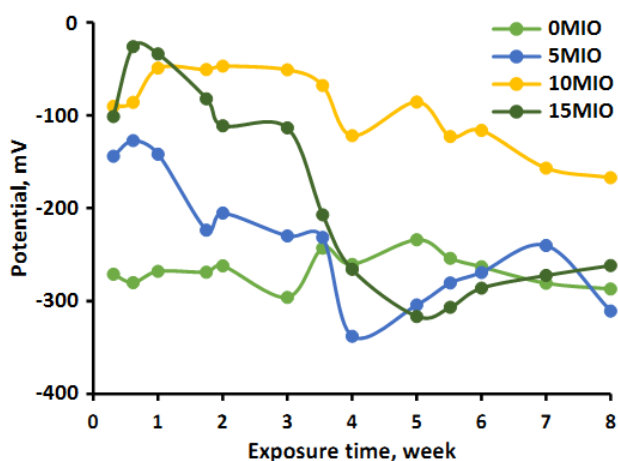


Figure 2. OCP versus exposure time of the coated steel reinforced concrete with different ER coatings containing MIO

The corrosion products may be shaped under the coatings in the existence of diffused electrolyte. Findings reveal the increase in OCP value of the blank specimen toward more positive values after 4 weeks of immersion. One probable reason for such observations is the formation of corrosion products in the metal/coating interface. Corrosion products have a high capacity for plugging

pores [16]. The pores plugging act by the corrosion products can lead to a reduction in the electrolyte diffusion rate into the metal/coating interface. However, a reduction in the OCP value may be observed again at exposure times bigger than 6 weeks. It can be attributed to two major causes. First, the corrosion product is deteriorated in the existence of chloride ions [17]. The deteriorated corrosion product has no more pore-plugging behavior. Second, the pore size (inside coating structure) enhances when the ER coating is immersed in aggressive electrolyte for long-term immersion [18]. It can be associated with hydrolytic degradation of the epoxy coating when it is immersed in the aggressive solution. When the ER was combined with MIOs, the OCPs were shifted toward positive values, as shown in Figure 1. The increase in OCP value becomes more apparent when the concentration of MIO into ER was 10 wt%. However, reduction in the OCP value was attained when the ER is incorporated with 15 wt% MIOs which can be related to the lower resistance of ER against permeation of electrolyte into the metal/coating interface. These findings can reveal the smaller electrolyte diffusion in the ER structure when it is incorporated with higher concentrations of the MIOs compared to the blank one. The increase in OCP value of the ERs incorporated with 10 wt% of MIOs can be found in Figure 2. At immersion times longer than 4 weeks, there is a reduction in the OCP value of the specimens reinforced with increasing MIOs content. It can be associated with hydrolytic degradation of ER at long-term immersion causing an enhancement in the amount of pores into the epoxy matrix. It can lead to an increase in diffusion of electrolyte into the metal/coating interface.

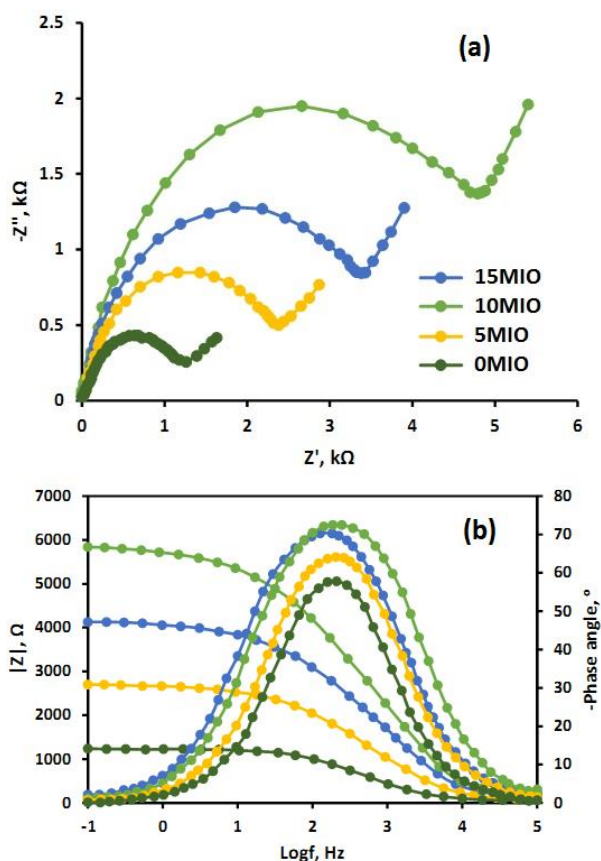


Figure 3. (a) Nyquist and (b) bode diagrams of the coated steel reinforced concrete with different ER coatings containing MIO immersed in 3.5wt% NaCl media after 8 weeks

Furthermore, the EIS assessment was used to study the corrosion resistance of steel rebars coated by ER containing the various concentrations of MIOs. Nyquist and bode plots of the specimens immersed in 3.5wt% NaCl solution after 8 weeks are indicated in Fig. 3. The Nyquist plots were fitted by a circuit model indicated in Fig. 3. The R_s , R_c , C_c , R_{ct} and C_{dl} are related to the solution resistance, coating resistance, coating capacitance, charge-transfer resistance and double-layer capacitance, respectively.

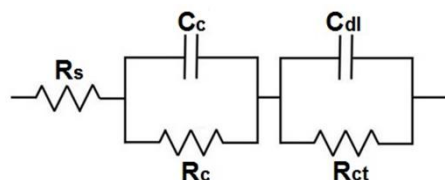


Figure 4. An equivalent circuit

Table 4 shows the values of various parameters achieved from the Nyquist diagrams. As shown, increasing the concentration of MIOs in ER coatings increased the R_{ct} of the samples compared to the blank ER. The maximum increase in R_{ct} was obtained for the sample which was incorporated with 10 wt% MIOs. In addition, the coating capacitance of the 10MIO sample was significantly lower than the other samples. When ER was incorporated by 10wt% MIOs, it revealed a higher coating resistance against electrolyte permeation. These findings are completely consonant with the OCP results. MIOs have a laminar form with the ability to produce barrier property against the permeation of electrolyte into the coating matrix. Actually, by using such particles, the length of the conduction paths within the coating matrix may be increased. It is clear that, MIOs because of their laminar form can create barrier effects against the permeation of electrolyte into the ER [19]. The impedance values improved when MIO amounts were raised in ER, as shown in figure 3b. According to this finding, the 10MIO sample effectively controls the corrosion of AISI 1045 Steel rebar in a marine environment. It is due to the ER fully covering the active surface of steel rebar. It can also be linked to the creation of a passivation film on the steel surface. Due to the formation of a protective passive film, the maximal phase-angle for an ER containing MIOs at a lower-frequency was moved to a higher angle [20], as seen in the figure 3b.

Table 4. The data obtained from fitting Nyquist curves for coated steel reinforced concrete with differentER coatings

Samples	R_s (Ω)	R_c ($k\Omega$)	$C_c(\mu Fcm^{-2})$	R_{ct} ($k\Omega$)	$C_{dl}(\mu Fcm^{-2})$	E (%)
0MIO	34	0.8	6.2	1.3	8.6	-
5MIO	29	1.8	4.7	2.7	6.8	51.8
10MIO	28	3.9	2.3	5.9	3.2	77.9
15MIO	35	2.7	3.3	4.2	4.7	69.0

The following equation was used to quantify efficiency (E):

$$E(\%)=100 \times (R_{ct}-R_{ct}^*)/R_{ct} \tag{1}$$

where R_{ct} and R_{ct}^* show charge-transfer resistance of samples with and without MIOs. Table 5 indicates the E comparison of epoxy coated steels as stated in literature. The results revealed that the E of 10MIO sample for corrosion resistance of AISI 1045 steel rebar was comparable with other reported epoxy coated steels.

Table 5. E comparison of epoxy coated steels as stated in literature

Epoxy coated materials	Environment	E (%)	Ref.
Epoxy glass flake	Marine	76.2	[21]
Epoxy/polyaniline-camphorsulfonate	chloride-laden	81.3	[22]
Enamel coatings	3.5 wt.% NaCl	83.7	[23]
Nanosilica-filled epoxy-resin	3.5wt% NaCl	79.4	[24]
Epoxy resin with MIO	3.5wt% NaCl	77.9	This work

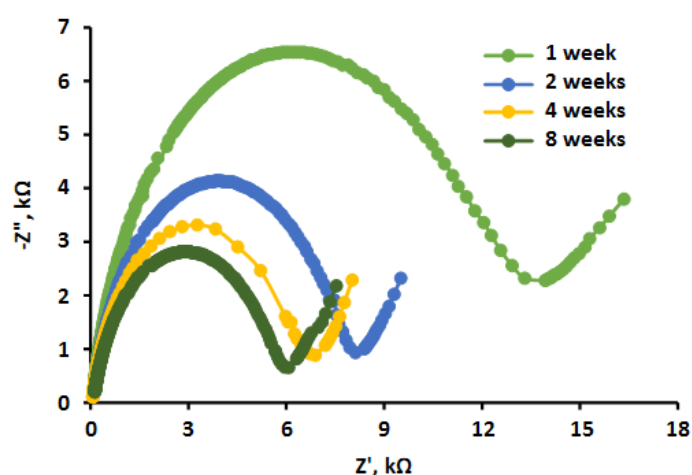


Figure 5. Nyquist diagrams of the 10MIO specimen immersed in 3.5wt% NaCl solution in different exposure times at room temperature

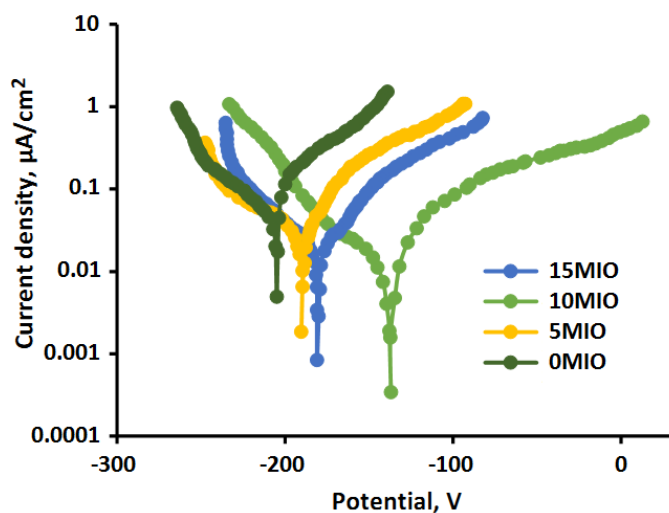


Figure 6. Polarization diagrams of steel rebars coated by ER containing the various concentrations of MIOs exposed to 3.5wt% NaCl media for 4 weeks at room temperature

The effect of immersion time on electrochemical corrosion behavior of the 10MIO sample was also considered by the EIS test at different exposure times (1, 2, 4 and 8 weeks). Figures 5 show the Nyquist diagrams of the specimens at different times. Due to the uniqueness of the Nyquist diagrams of the mentioned samples, the simple equivalent circuit of Figure 4 was used to analyze the impedance spectra. As shown in the Nyquist diagrams, over time, the capacitive arcs become smaller, indicating the penetration. Gradually, after 8 weeks of immersion of the coatings, as shown in Figure 5, the 10MIO sample has the greatest drop in resistance, indicating easier penetration of water molecules and aggressive ions into the coating.

The polarization curves of steel rebars coated by ER containing the various concentrations of MIOs immersed in 3.5wt% NaCl media for 4 weeks are indicated in Figure 6. The obtained corrosion parameters are shown in table 6.

Table 6. Corrosion parameters of steel rebars

Samples	Corrosion current density ($\mu\text{A}/\text{cm}^2$)	Corrosion potential (mV)
0MIO	0.223	-212
5MIO	0.097	-187
10MIO	0.064	-138
15MIO	0.036	-176

The MIO-free sample had the minimum value of corrosion potential in comparison with the other samples. The coated steel rebar embedded in concrete was in a state of passive and was a lower prone to corrosion. As exhibited in figure 6, the addition of MIOs results in a significant enhancement in corrosion potential. As a result, the potential has a higher positive value. Furthermore, its corrosion current density also changed to the left, indicating that the reinforcement bars surface has very little corrosion current [25]. The corrosion levels may be introduced in four levels prepared by Durar Network Specifications [26]. The corrosion current of sample 10-MIO in 3.5wt% NaCl medium, on the other hand, was lower than that of the other specimens. Hence, except the MIO-free sample, all coated steel rebars stayed at the passive level in the experiment procedure which exhibited their excellent resistance to corrosion of AISI 1045 steel in marine medium.

Figure 7 exhibits the surface morphology of steel rebars with epoxy coatings with MIO-free and 10 wt% MIO immersed to 3.5wt% NaCl media for 4 weeks. Fig. 7b displayed that the 10-MIO sample is more uniform and smooth than the MIO-free sample and have low-pitting corrosion onto steel surface, which agrees with previous reports. Actually, reduced pores and capillary porosity in MIO-enhanced epoxy coatings cause less permeability of chloride ions on steel surfaces, resulting in less corrosion production.

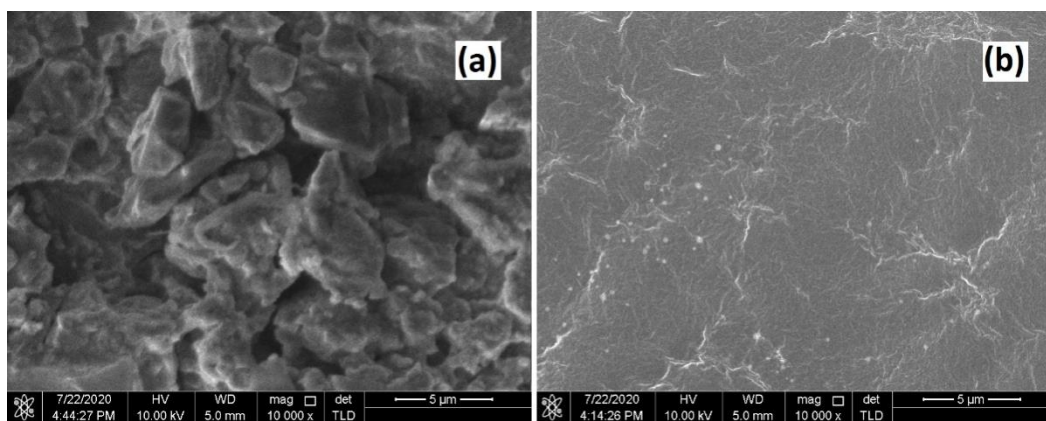


Figure 7. Surface morphology of steel rebars with various epoxy coatings (a) MIO-free, (b) 10-MIO samples immersed to 3.5wt% NaCl media for 4 weeks

4. CONCLUSIONS

In this study, different ratios of MIO pigments were added to the structure of ER-based primer coatings. The prepared coating materials were applied to samples of AISI 1045 steel rebars with 8 mm diameter and their corrosion resistance was investigated using EIS and polarization tests. The corrosion potential and resistance of steel rebars coated with ER containing 10 wt% MIOs (10MIO) were found to be higher than the other samples in the EIS. Polarization results exhibited that except the MIO-free sample, all coated steel rebars stayed at the passive level in the experiment procedure which exhibited their excellent resistance to corrosion of AISI 1045 steel in marine medium. The surface morphology of coated steel rebar showed that the 10MIO sample had less pitting corrosion than the other tests, which matched the electrochemical findings.

References

1. P. Pokorný, P. Tej and M. Kouřil, *Construction and Building Materials*, 132 (2017) 271.
2. M. Feizbahr, S.M. Mirhosseini and A.H. Joshaghani, *Express Nano Letters*, 1 (2020) 1.
3. C. Xiong, W. Li, Z. Jin, X. Gao, W. Wang, H. Tian, P. Han, L. Song and L. Jiang, *Corrosion Science*, 139 (2018) 275.
4. F. Qu, W. Li, W. Dong, V.W. Tam and T. Yu, *Journal of Building Engineering*, 15 (2020) 102074.
5. X. Zhao, L. Cheng, N. Jia, R. Wang, L. Liu and C. Gao, *Journal of Membrane Science*, 600 (2020) 117857.
6. M. Yasir, F. Ahmad, P.S.M.M. Yusoff, S. Ullah and M. Jimenez, *Surface Engineering*, 36 (2020) 334.
7. C.M. Senna, D. Santos and T.S. Geraldi, *International Journal of Advanced Engineering Research and Science*, 5 264288.
8. M. Feizbahr, J. Jayaprakash, M. Jamshidi and C. Keong, *Middle-East Journal of Scientific Research*, 13 (2013) 1312.
9. Z. Ding, L. Yuan, G. Liang and A. Gu, *Journal of Materials Chemistry A*, 7 (2019) 9736.

10. R. Unger, U. Braun, J. Fankhänel, B. Daum, B. Arash and R. Rolfes, *Computational Materials Science*, 161 (2019) 223.
11. Y. Zhang, *International Journal of Electrochemical Science*, 14 (2019) 9347.
12. Q. Xiang and F. Xiao, *Construction and Building Materials*, 235 (2020) 117529.
13. T.A. Truc, N.X. Hoan, T.T. Thuy, K. Ramadass, C. Sathish, N.T. Chinh, N.D. Trinh and T. Hoang, *Journal of nanoscience and nanotechnology*, 20 (2020) 3519.
14. A. Akbari, M. Nikookar and M. Feizbahr, *Research in Civil and Environmental Engineering*, 1 (2013) 287.
15. T. Srichumpong, S. Angkulpipat, S. Prasertwong, N. Thongpun, C. Teanchai, P. Veronesi, K. Suputtamongkol, C. Leonelli, G. Heness and D. Chaysuwan, *Journal of Non-Crystalline Solids*, 528 (2020) 119730.
16. M. Talebian, K. Raeissi, M. Atapour, B. Fernández-Pérez, A. Betancor-Abreu, I. Llorente, S. Fajardo, Z. Salarvand, S. Meghdadi and M. Amirnasr, *Corrosion Science*, 160 (2019) 108130.
17. Y. Reda, A. El-Shamy, K. Zohdy and A.K. Eessaa, *Ain Shams Engineering Journal*, 11 (2020) 191.
18. Z. Chen, W. Yang, X. Yin, Y. Chen, Y. Liu and B. Xu, *Progress in Organic Coatings*, 146 (2020) 105750.
19. A. Ali, M. Aamir, K.H. Thebo and J. Akhtar, *The Chemical Record*, 20 (2020) 344.
20. H.-S. Ryu, J.K. Singh, H.-S. Lee, M.A. Ismail and W.-J. Park, *Construction and Building Materials*, 133 (2017) 387.
21. W. Tian, L. Liu, F. Meng, Y. Liu, Y. Li and F. Wang, *Corrosion Science*, 86 (2014) 81.
22. S. Pour-Ali, C. Dehghanian and A. Kosari, *Corrosion Science*, 90 (2015) 239.
23. F. Tang, G. Chen, R.K. Brow, J.S. Volz and M.L. Koenigstein, *Corrosion Science*, 59 (2012) 157.
24. M. Conradi, A. Kocijan, D. Kek-Merl, M. Zorko and I. Verpoest, *Applied Surface Science*, 292 (2014) 432.
25. Z. Jin, H. Chang, F. Du, T. Zhao, Y. Jiang and Y. Chen, *Corrosion Science*, 171 (2020) 108714.
26. M.A. Baltazar-Zamora, H. Ariza-Figueroa, L. Landa-Ruiz and R. Croche, *European Journal of Engineering and Technology Research*, 5 (2020) 353.